Available online www.jsaer.com

***Journal of Scientific and Engineering Research*, 2023, 10(12):107-119**

Research Article

ISSN: 2394-2630
CODEN(USA): JSERBR

Evaluation of Direct Solar Radiation by the Kasten Model Compared to Online Pvgis Data around the Sonichar Clinker Burial Center in Tchirozérine

Seydou DJIKA[1], Boubou BAGRE[2], Harouna SANI DAN NOMAO[1], Makinta BOUKAR[1*], Saïdou MADOUGOU[1]

[1]Laboratoire d'Energétique et d'Electronique d'Electrotechnique, d'Automatique, d'Informatique Industrielle (LAERT-LA2EI), Université Abdou Moumouni de Niamey
[2]WASCAL, Université Abdou Moumouni de Niamey
*Corresponding autor : Makinta BOUKAR
*Email: makintag@gmail.com

Abstract This study consists of evaluating the thermodynamic solar potential in the surroundings of the SONICHAR clinker burial center in Tchirozérine.

This consists of determining the direct solar radiation because it is the only parameter used for the sizing of the thermodynamic concentrated solar power plant.

The irradiation of approximately 2500 kWh/m^2/year obtained at the end of this research shows that this region located in the north of Niger republic is favorable for the installation of this technology. The sun appears all 12 months of the year. This solar deposit in the area, although very important, is currently unexploited, while the country is facing a major energy problem.

Its exploitation can be an alternative to the recurring electricity problem experienced by Niger republic in general and the Agadez region in particular.

Keywords concentrator, radiation, solar, thermodynamics, clinker

1. Introduction

Solar radiation in a sunny region is of the order of 1 kW/m^2 of power, and the earth can receive per year approximately 14,000 times the world's energy consumption (400.10^{18} Joules) in the form of solar radiation and 2/3 of this radiated energy reaches ground level under good sunlight conditions [1-2]. To harness this energy from the sun with the aim of generating electricity; two methods were favored: photovoltaics (PV) which is the conversion of photons into electricity and thermodynamic solar which is the conversion of heat into work then into electricity through a CSP concentration system. Of these two solar electricity production systems, photovoltaics is a limited solution given the high cost of the storage system with a short battery life (3 to 7 years on average) while thermodynamic solar technology offers the possibility storage [3-4] of heat which in turn allows the production of electrical energy continuously (day and night time) with good efficiency and economical and robust technology [5]. Currently and for the years to come, energy production is a challenge of great importance for the energy needs of industrialized societies in general and in particular for developing countries like ours (Niger republic).

Niger republic is one of the least developed countries (LDCs) [6-7]. With an area more than twice that of France, around 80% of Niger's republic territory is covered by desert and 85% of its population is rural, of which the number of people living in this desert part is estimated at around one million [8]. Poverty, insecurity,

climate and immensity of Nigerian territory are important factors that slow down the development of the national electricity sector. As a result, Niger republic is one of the lowest electrified countries in Africa with less than 15 % of the population who benefits from access to electricity [9-10].

In view of the above, Niger must consider diversifying its electrical energy production system by introducing thermodynamic concentrated solar technology in order to take the maximum benefit from this system which uses solar radiation. The production principle is to concentrate the heat of the sun through mirrors to heat a fluid to high temperature in order to generate steam by heat exchange and then produce electricity by means of a turbine [11-12].

The objective of this work is to evaluate the direct solar radiation (DNI) either by exploitation of satellite data, or by calculation through semi-empirical equations using geographical data of the location, with a view to the installation of a solar thermal power plant near the SONICHAR clinker burial center using ceramic balls in the storage system [13-14].

2. Materials and Methods

The site of this study is located in TCHIROZERINE, capital of the department of the same name, located as the crow flies approximately 45 km northeast of the urban commune of AGADEZ [15]. The coordinates of this site are 17°16.45'2" north latitude and 7°51'28.4" east longitude. This site covers an area of 50,539 km² and is located 517 m above sea level.

The methodology adopted consists of using the method of LIU - JORDAN (1960) in which the number n of the day of the year appears (table 1). It consists of taking the 16th day of each month as the most representative of the average day of the month considered [2]. As for Klein (1979), he showed that it was preferable to choose this day using table 1, which gives the estimate of the number of the day of the year to be considered in the calculation. We then evaluate, based on the site's basic data, the instantaneous direct illumination for each month by carrying out 13 operations in steps from 6 a.m. to 6 p.m. The year 2020 was taken as a reference for measurements with the PVGIS software while respecting one-hour steps between 6 a.m. and 6 p.m.

Table 1: Estimated day number of the year, according to Lui-Jordan and Klein

Month	Day number in the month	Day number of the year
January	17	17
February	16	47
March	16	75
April	15	105
May	15	135
June	11	162
July	17	198
August	16	228
September	15	258
October	15	288
November	14	318
December	10	344

To obtain the instantaneous direct radiation, simply enter the time at which you wish to calculate this irradiation. Knowing that the length of the day is automatically calculated, we can deduce the average monthly radiation by integrating the energy received during the day. As a first approximation, the daily radiation curve can be assimilated to a portion of a sinusoid whose area represents the average irradiation obtained by the integration:

$$DNI_{moy} = \frac{2}{T}\int_0^{T/2} I_{max} \sin\left(\frac{2\pi}{T}t\right) dt = \frac{2I_{max}}{\pi} \quad (1)$$

The direct average irradiation is then obtained by:

$$E = DNI_{moy}\ X \text{ daily sunshine duration} \quad (2)$$

This formula allows you to calculate the DNI for each month. It is this parameter which is used in concentration sensors.

2.1 Error calculation

Measuring stations are rare across the national territory. To this end, for the estimation of incident solar irradiation, theoretical models or satellite data are used, although most satellites are not intended to collect African data [16]. These are models established in the form of correlations. To apply them to the sites considered, the calculated solar lights will be faced with other values measured on the site by other applications during any period.

For each day considered, we have on the one hand drawn up on the same diagram, the curves representative of the values recorded by PVGIS and those estimated by the Kasten model and on the other hand, we have calculated the average relative difference between the values noted and those estimated by the model. The comparison was carried out on the direct solar irradiance of 12 days corresponding to the 12 months of the year in accordance with the requirements of Table 1. We calculate in our case, the relative root mean square error (RMSE) and the average relative error (ERM) [16-17]. These differences are calculated by the following relationships:

$$RMSE = \frac{\sqrt{\sum_{i=1}^{n}[I(recorded)-I(calculated)]^2}}{\sum_{i=1}^{n} I(recorded)} x100 \quad (3)$$

$$ERM = \frac{\sum_{i=1}^{n} I(recorded)-I(calculated)}{\sum_{i=1}^{n} I(recorded)} x100 \quad (4)$$

The direct radiation obtained by PVGIS was taken as the reference value (given value).

2.2 PVGIS satellite data

A meteorological satellite is an artificial satellite whose main mission is to collect data used for monitoring the earth's weather and climate. There are several satellite data sites. For this study, the PVGIS (Photovoltaic Geographical Information System) site was used. It is the PVMAPS software that provides access to all the estimation models used in PVGIS. The daily average solar irradiation data can be retrieved in the form of a table usable in any other software and in the form of graphs presenting annual values. The data is obtained via this online software PVGIS. [https://re.jrc.ec.europa.eu/pvg_tools/fr/tools, 06 08 2021, 3:20 p.m.]

We had access to PVGIS data through 2020 to determine normal direct irradiation.

2.3 Calculations of direct irradiation from geographic data of the clear sky location

The direct irradiance in a plane perpendicular to the sun is given in W/m² by the KASTEN formula:

$$I = (I_0 - 31T_1) \times \exp\left(-\frac{m_h \times T_1}{0{,}9 \times m_h + 9{,}4}\right) \quad (5)$$

With I_0 solar constant $I_0 = 1368\, W.m^{-2}$ [18]

m_h: called atmospheric mass or optical distance defined from the unit of atmospheric thickness taken vertically at zero level, and calculated as follows:

$$m_h = \frac{P_m}{1013} \frac{(0{,}88)^z}{sin(h)} \quad (6)$$

P_m Atmospheric pressure in mbar and altitude z in km.

T_L: Linke disorder factor; It leads to an evaluation of atmospheric extinction by gaseous molecules and aerosols. It can be calculated by the formula:

$$T_L = 2{,}5 + 16 \times BA + 0{,}5 \times ln(\omega'') \quad (7)$$

ω': Height of condensable water.

BA: Angstrom coefficient.

The Angstrom coefficient is defined from the number of aerosols contained in the atmospheric mass, unit placed vertically at the measurement location (depending on the clarity of the sky), with the height of condensable water. These coefficients are presented in Table 2.

Table 2: Number of aerosols contained in the atmospheric mass

Nature of sky	Water height $\omega'(cm)$	Angstrom Coefficient BA
Degraded sky (dust and aerosols)	5	0,2
Average sky	2	0,1
Clear sky	1	0,01

The component of direct radiation on a horizontal surface is then, in all cases:

$$I_h = I \times \sin h \quad (8)$$

For a flat surface inclined at an angle i relative to the horizontal and oriented towards a direction making an angle γ with the south (γ counted positively towards the West), equation (6) becomes:

$$I(i,\gamma) = I \times [cos\,(h) \times sin\,(i) \times cos\,(a - \gamma) + sin\,(h) \times cos\,(i)] \quad (9)$$

With a azimuth; the angle that the projection of the direction of the star makes on the horizontal plane (plane tangent to the ground) with the south direction.

Azimuth (a): Gauss's formula gives this angle:

$$cos\,(h) \times sin\,(a) = sin\,(\omega) \times cos\,(\delta) \quad (10)$$

Length of day (LOD)

$$LOD = \frac{2}{15} \times [arc\,cos\,(-tg(\delta) \times tg(\varphi))] \quad (11)$$

3. Results and Discussions

3.1 Error curve versus time

Visual inspection makes it possible to exclude values that are likely abnormal or suspicious, such as values distorted by shadows or clouds on the sensors or the incorrect position of the shading ring [19]. After this check on the available irradiations, the percentages of values to exclude are the RMSE and ERM (figure 1) of the typical day of the month of July which are respectively 203.94% and 105.49%. These values are certainly due to bad weather during the winter period or to the strong dust winds which are very frequent in the area and which made it possible to record low radiation values with PVGIS.

But nevertheless we obtain the average value of RMSE of 28.40% and that of ERM at 19.58%. These errors show that these two methods give results with a considerable difference.

There is reason to consider another evaluation with other models in order to determine the most acceptable models.

On the other hand, in Figure 2 we have plotted the evolution curve of the ERM of direct solar radiation DNI over the 12 months with the two methods. We see that its value is around 10% except in the month of September when the radiation reading with PVGIS was very low which led to an error difference on the DNI of more than 30%. We can admit that these two methods make it possible to obtain values sufficiently close to the DNI.

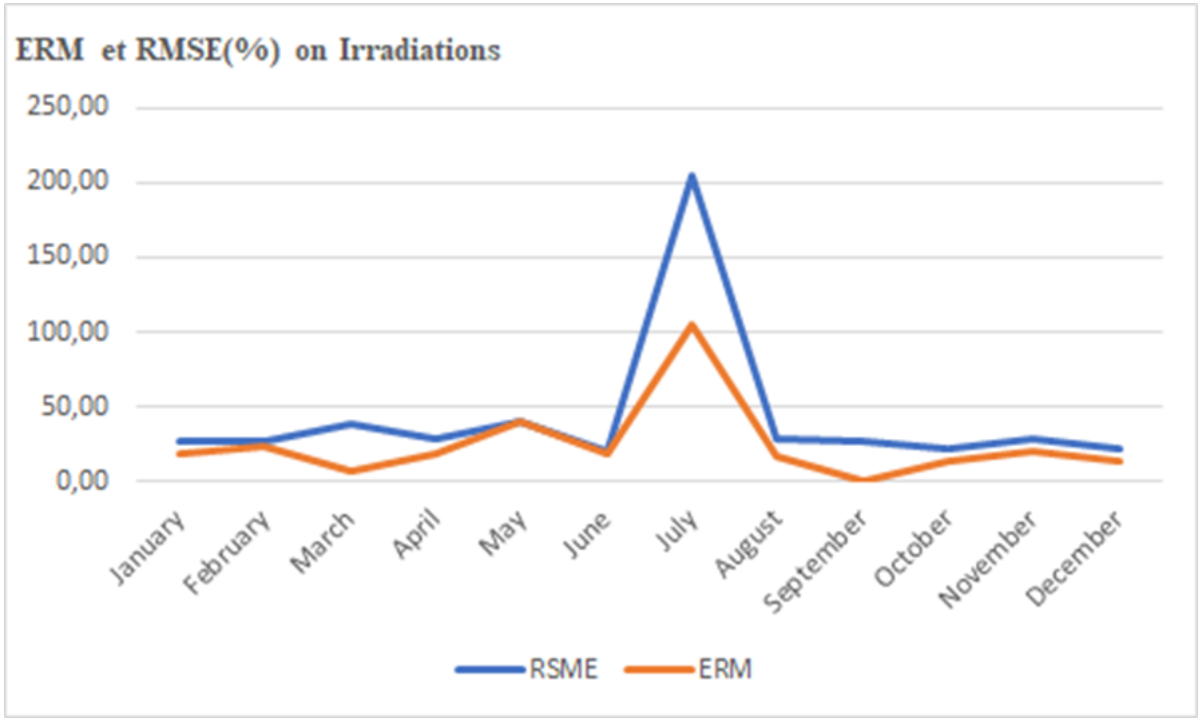

Figure 1: Evolution curve of RMSE and ERM errors on irradiations

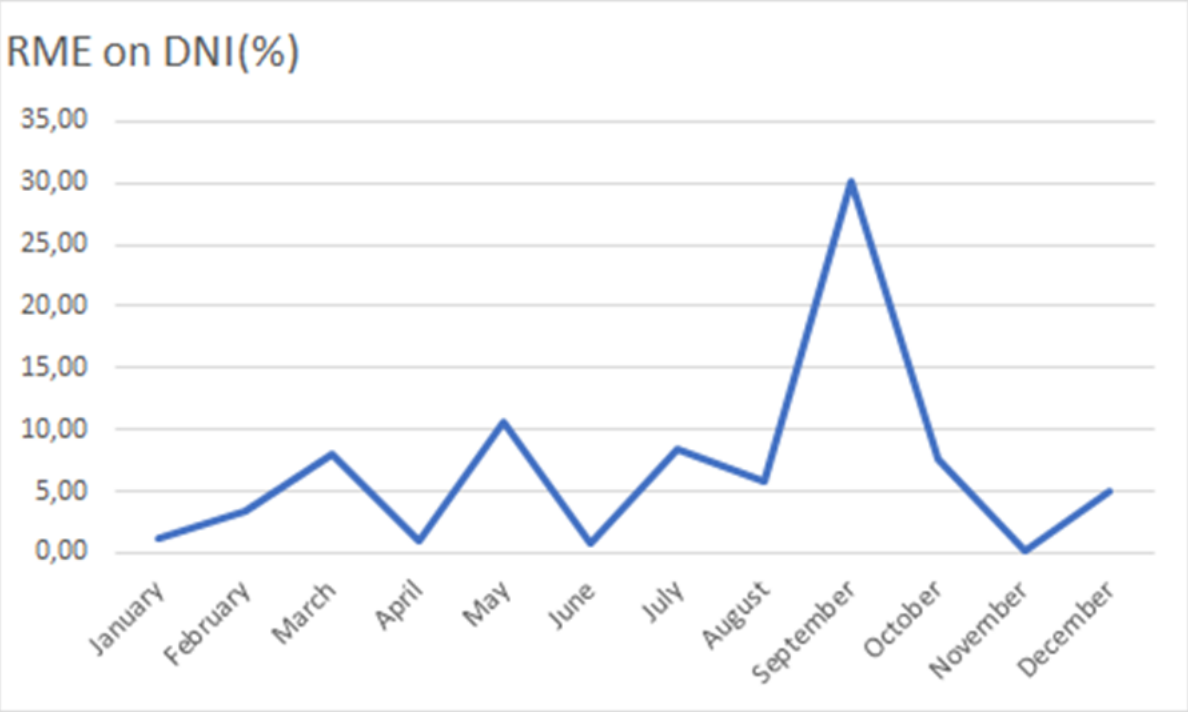

Figure 2: Error evolution curve on the DNI

3.2 Direct solar irradiations obtained by the two methods

By applying equation 5 (KASTEN method) to the 12 months of the year on the basis of the number of the day of the year corresponding to the month (table 1), we arrive at the results on the evolution of daily irradiations of each month (figures 3). They have the appearance of a half-sinusoid. These are results obtained by reading (PVGIS) and by calculation (Kasten Model) from 6 a.m. until 6 p.m. in one-hour increments. We observe that this magnitude reaches its maximum between 12 p.m. and 1 p.m. for each month where it reached a peak of 919.28 W/m^2 at 12:10 p.m. in the month of October.

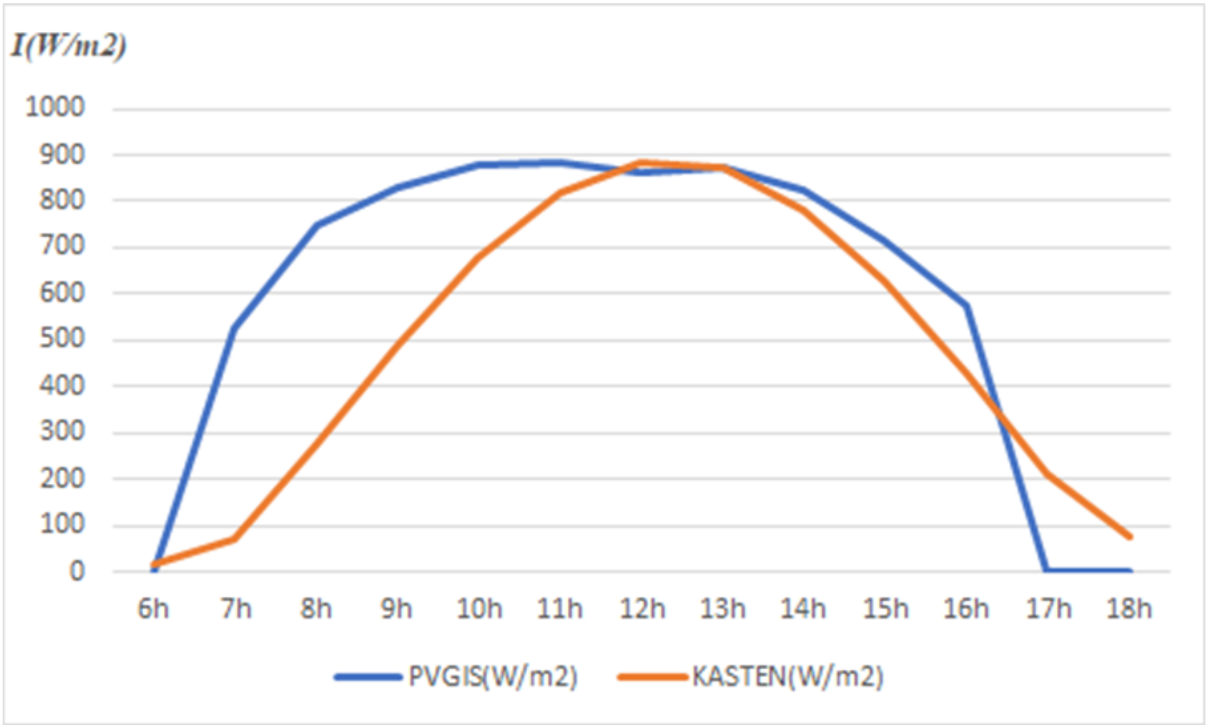

Figure 3: Curve of the evolution of the irradiation of the day in January

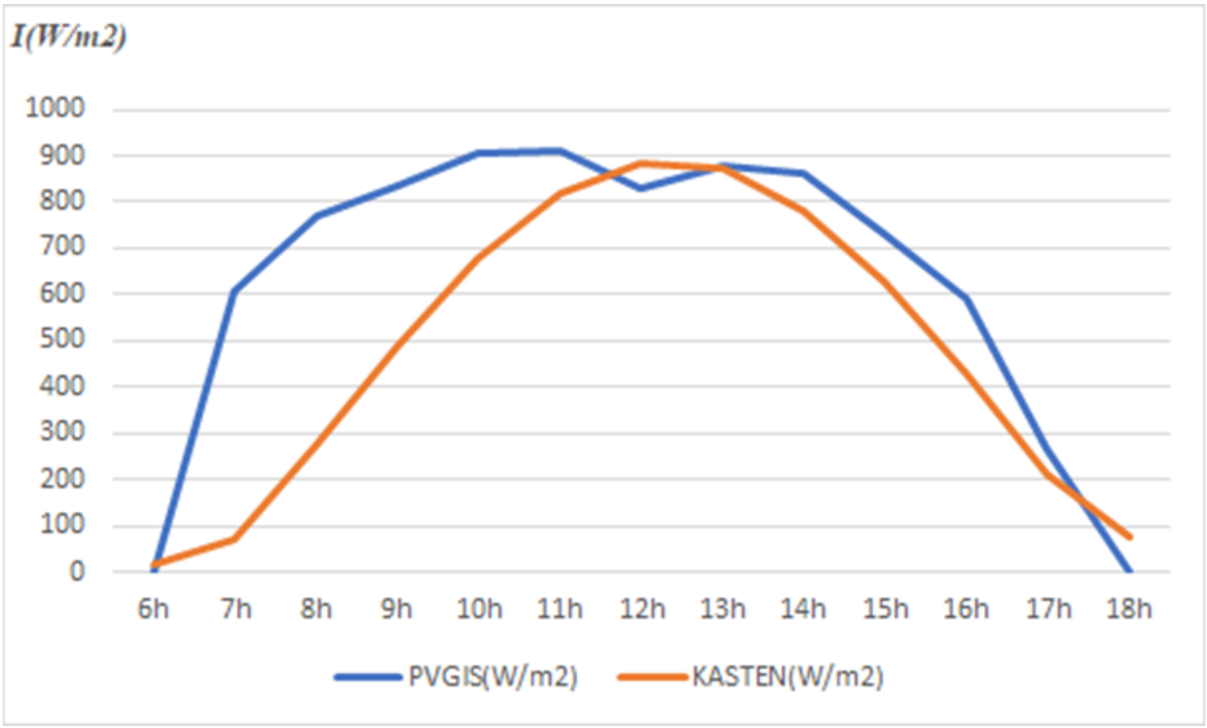

Figure 4: Curve of the evolution of the irradiation of the day in February

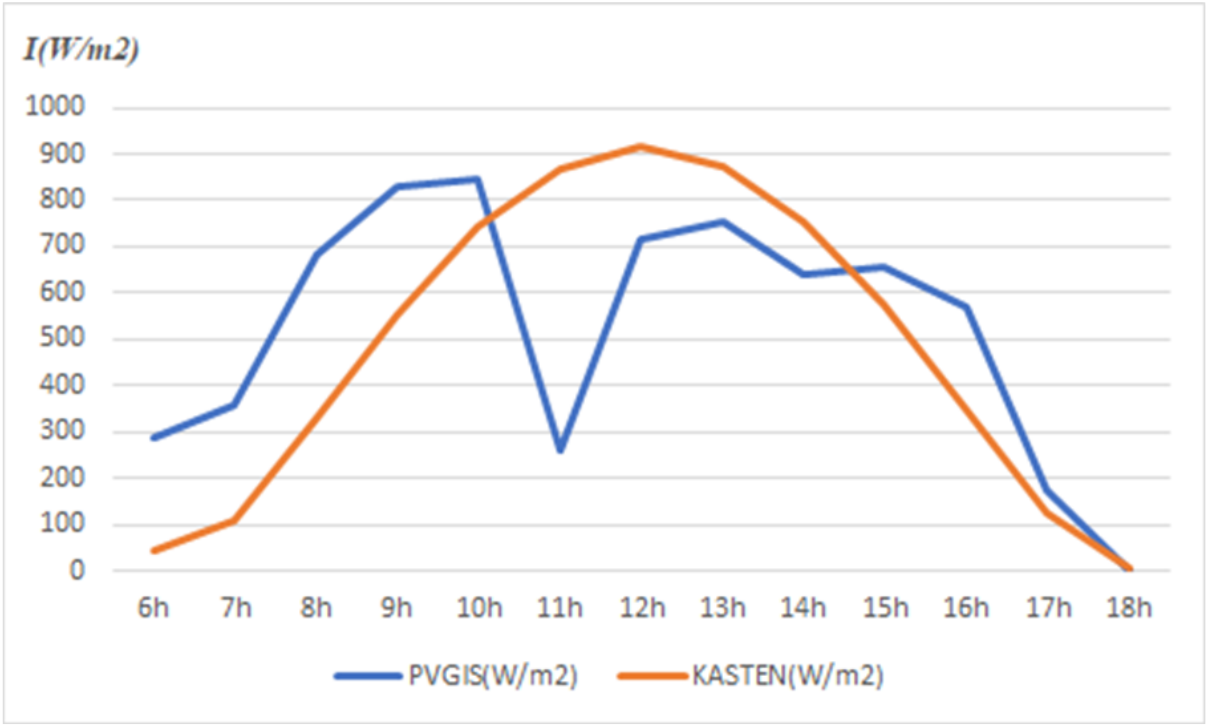

Figure 5: Curve of the evolution of the irradiation of the day in March

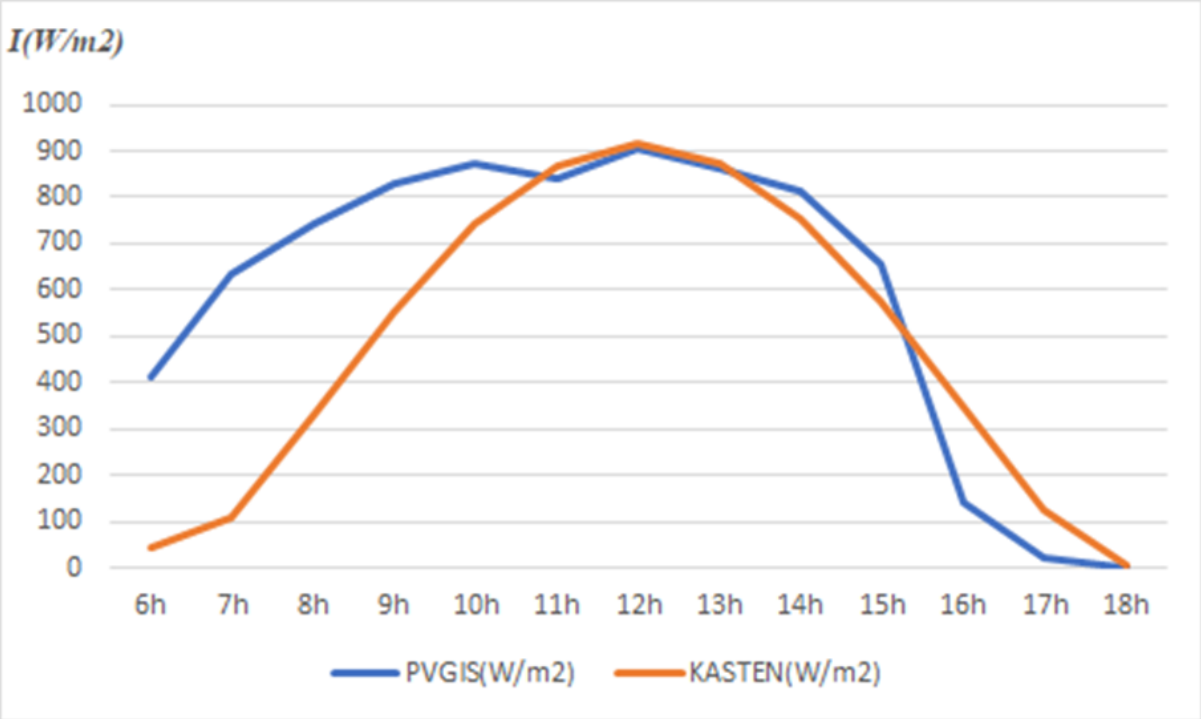

Figure 6: Curve of the evolution of the irradiation of the day in April

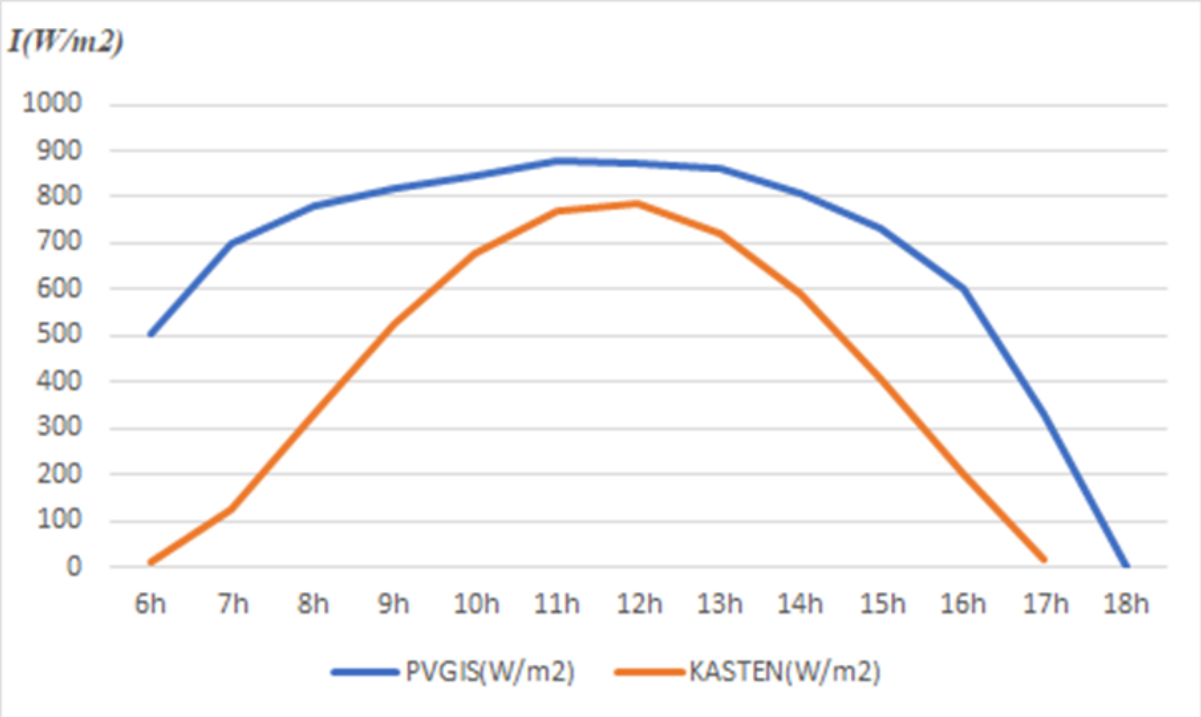

Figure 7: Curve of the evolution of the irradiation of the day in May

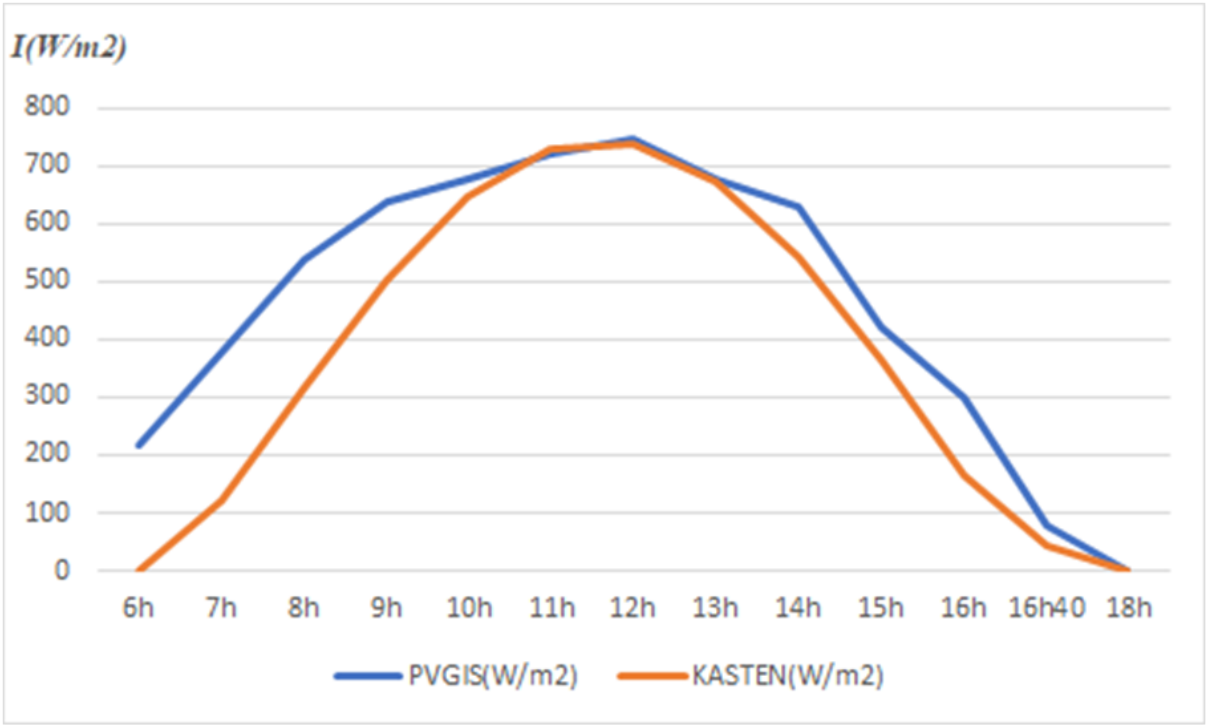

Figure 8: Curve of the evolution of the irradiation of the day in June

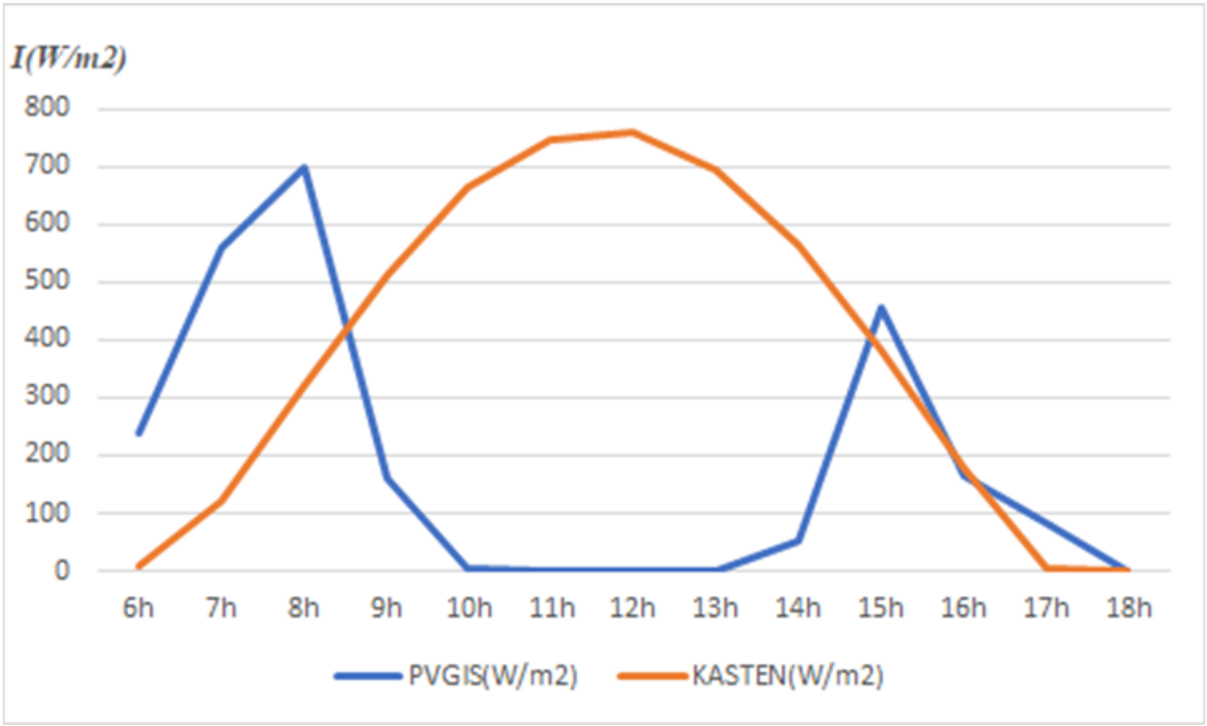

Figure 9: Curve of the evolution of the irradiation of the day in July

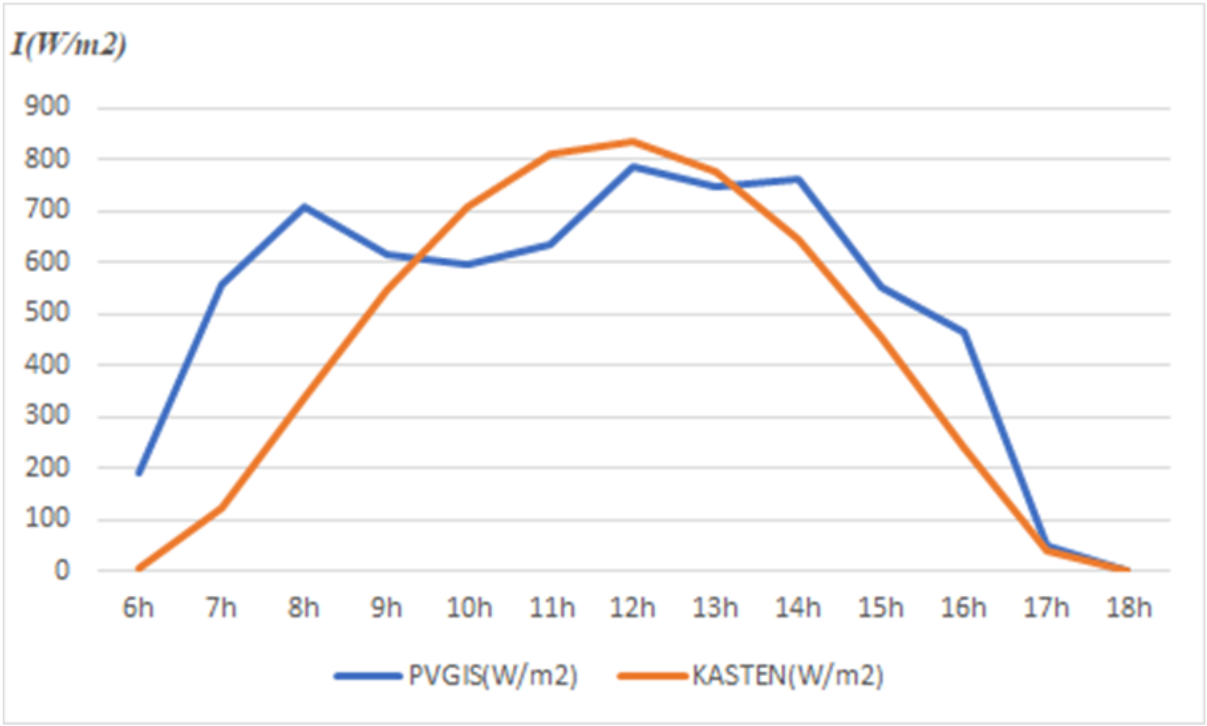

Figure 10: Curve of the evolution of the irradiation of the day in August

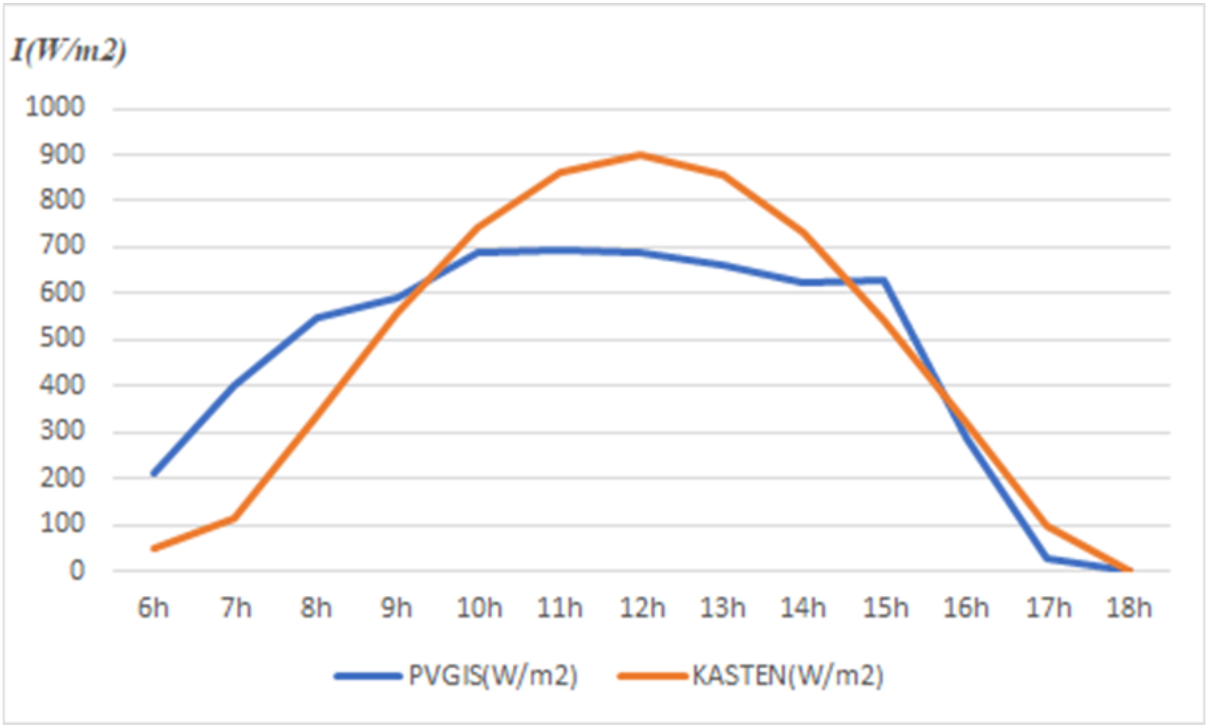

Figure 11: Curve of the evolution of the irradiation of the day in September

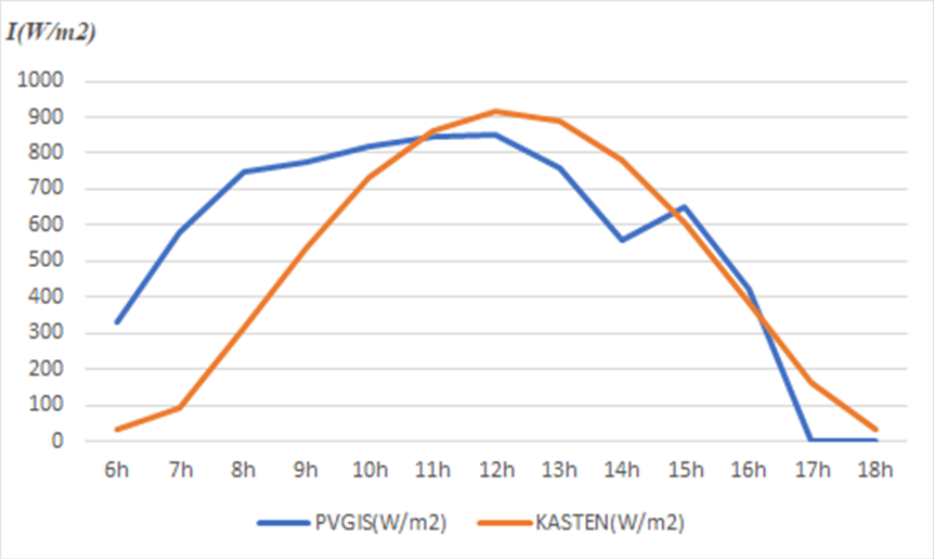

Figure 12: Curve of the evolution of the irradiation of the day in October

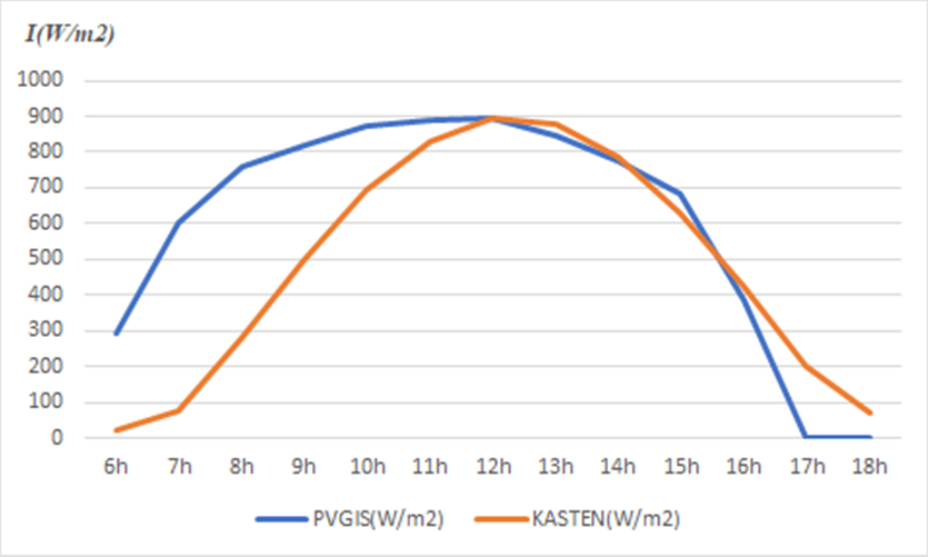

Figure 13: Curve of the evolution of the irradiation of the day in November

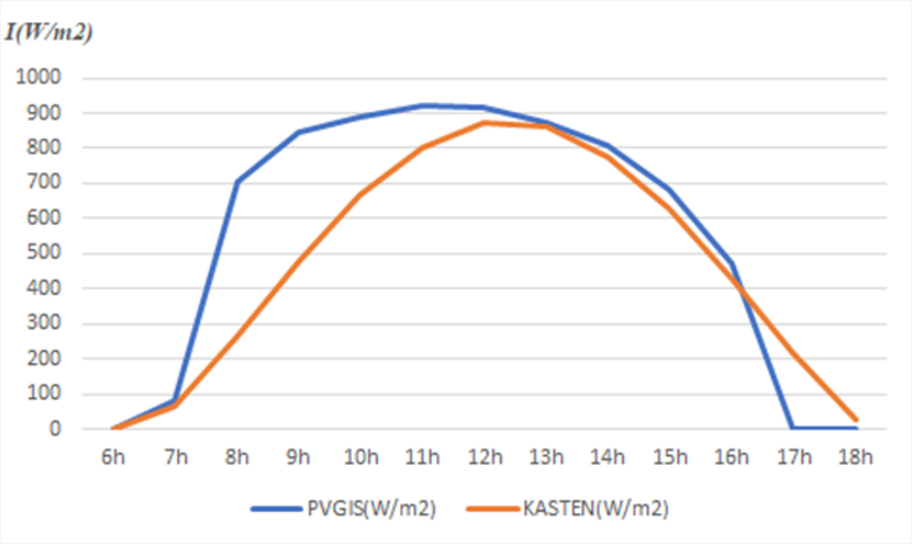

Figure 14: Curve of the evolution of the irradiation of the day in December

From the diagrams representing the values obtained in Figures (3 to 14), we note that over the 12 months the readings with PVGIS are always overestimated from sunrise, generally around 7 a.m. Sometimes at 6 a.m., we record 0 W/m^2 while at 7 a.m. we can obtain a value beyond 600W/m^2. This may be the optical path effect, which appears near sunrise [20]; hence the recording of imprecise values. For these conditions, errors can exceed 50%. Which generally leads to significant discrepancies.

All the curves resulting from the Kasten model have the shape of a half-sinusoid. This is due to the fact that we have considered not only the direct illuminance (I) for the clear sky but also no cloudiness is taken into account.

On the other hand, those obtained with PVGIS, some have the shape of a half sinusoid with irregular points but most do not even present a maximum irradiation in the expected interval (between 0 p.m and 1p.m.). During the day in March (i.e. March 16 or the 75th day of the year) we observe a sudden drop in radiation around 11 a.m. with the PVGIS reading. This can be explained by the fact that it is a desert area with a wind of dust and sand that can appear at any time and create a mask on the site. On the other hand, during the day in July (March 17 or the 198th day of the year), still with PVGIS, we observe an extinction of sunshine from 10 a.m. to 2 p.m. This can be explained by the fact that the hibernal period extends over two months of the year (July to August).

Length of day (h)

The use of the Kasten model made it possible to determine not only daily and monthly irradiations but also the daily duration of sunshine.

Considering the 16th day as the most representative of the average day of the month considered, equation 9 makes it possible to determine this length of day of each month and to trace its evolution in Figure 15.

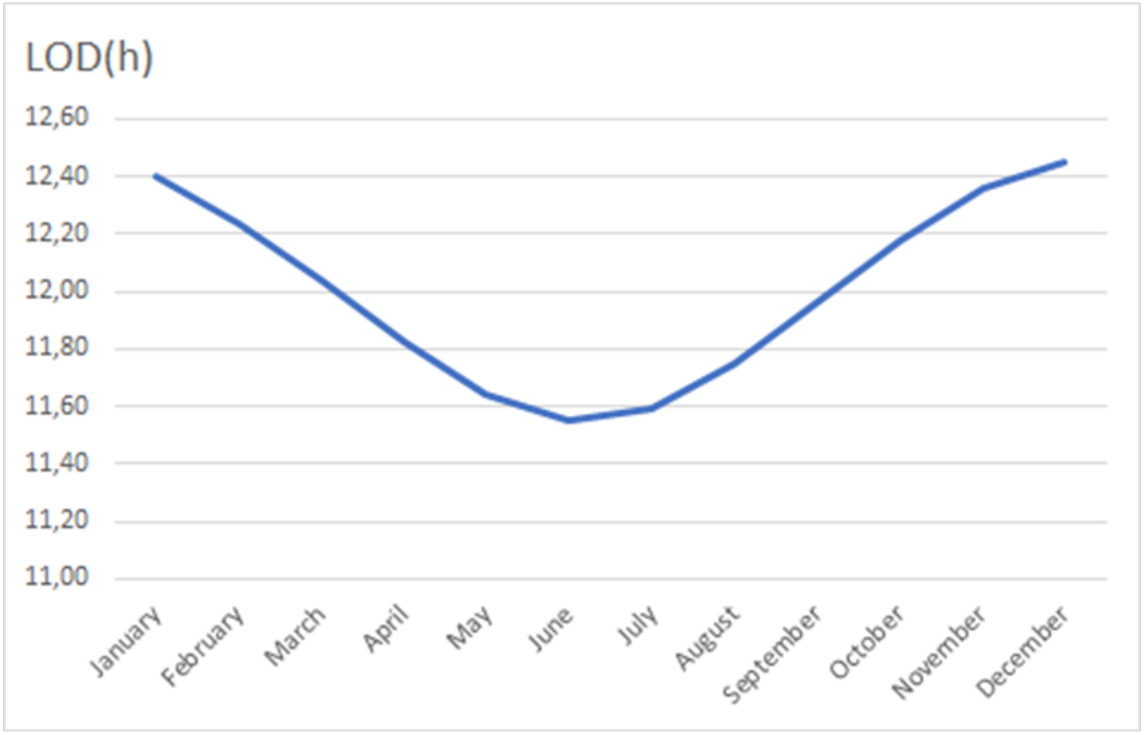

Figure 15: Day length evolution curve

From this curve, the longest days are observed in November, December and January while the shortest are observed in May, June and July.

Estimation of irradiation (kWh/m^2)

By applying equation 2 to the monthly averages of the DNI obtained, we calculated the irradiations for each month. This allows us to observe the evolution of these irradiations by the two methods in Figure 16.

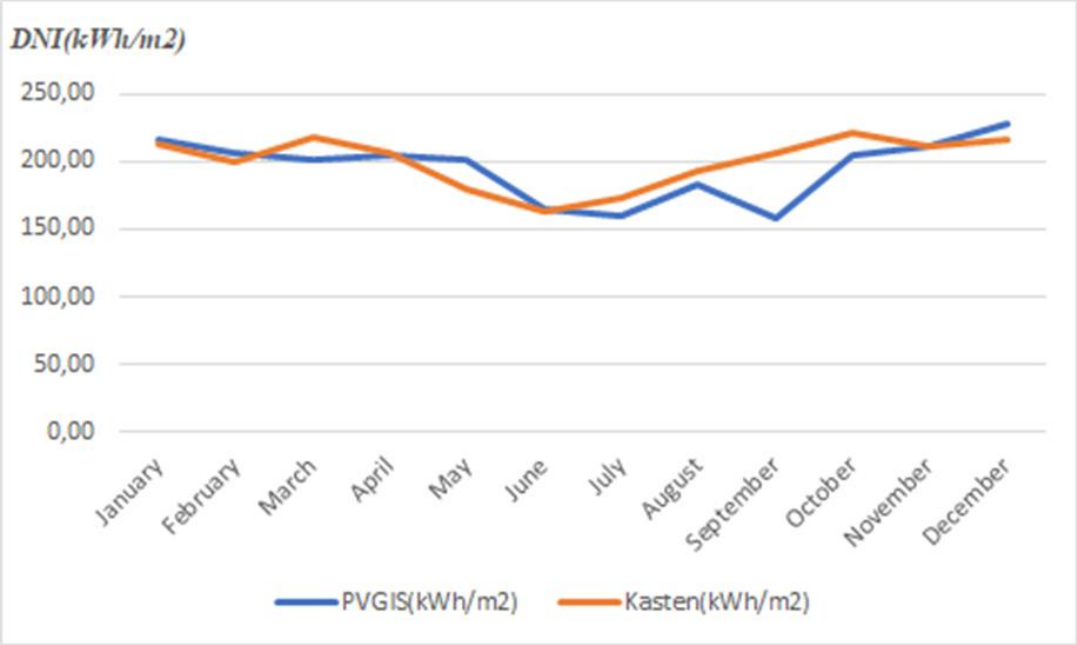

Figure 16: Annual evolution of average direct radiation

We observe that the DNI values are noticeably very close throughout the year except in October when there appears a slight difference between the two methods. This can be explained by the fact that the Kasten model considers a clear sky whereas in the desert zone at any time winds of dust or sand can appear.

Table 3 summarizes the results of these two DNI evaluation methods, which results in an annual average value of 2337 kWh/m^2 with PVGIS and 2399 kWh/m^2 with the KASTEN model. These methods give a satisfactory result [21].

Table 3: annual DNI summary

Methods	**PVGIS**	**KASTEN model**
DNI (kWh/m^2/year)	2337	2399

Although these two methods gave disparate daily and monthly irradiations, we ended up with almost identical annual direct radiation values.

4. Conclusion

The exploitation of energy produced by solar radiation continues to develop. Lack of knowledge of the technology by decision-makers, the financial costs of installation and the meteorological problem are factors that slow down its exploitation. Niger, being a Sahelian country with strong solar potential, receives sufficient thermal energy from the sun [22] to respond to the recurring problems of power cuts which is one of the major factors of its underdevelopment.

At the end of the research carried out, we note that the shortest duration of sunshine is 11:33 a.m. and can reach up to 12:27 p.m. in at times.

We determined the thermodynamic solar potential in the vicinity of the SONICHAR clinker burial site with the calculation method using the KASTEN model and the values measured by satellites and stored on the PVGIS databases.

This study showed that this region of Niger is favorable to the exploitation of this inexhaustible energy source which is thermodynamic solar energy with an irradiation value of 2337kWh/m^2 with PVGIS and 2399 kWh/m^2 with the model of Kasten per year.

These results could be considered as a database for the technico-economic evaluation of thermodynamic solar power plants in the AGADEZ region.

References

[1]. Benbouza Naima; 2008; Etude du rayonnement solaire dans la région de Batna ; Mémoire de Magister en Electrotechnique Option : Maîtrise des Energies ; p98

[2]. Frédéric LIVET (SIMaP, UMR CNRS 5266, INPG-UJF, BP 75 38402-St Martin d'Hères, France); 2011; Le solaire thermique à concentration
[3]. Mr Abdelmadjid KADDOUR; 2013; Modélisation et simulation d'un concentrateur parabolique solaire à moteur Stirling en vue d'un rendement optimal; Thèse UNIVERSITE ABOU-BEKR BELKAID-TLEMCEN; P 114
[4]. Mancini T, Heller P, Butler B, Osborn B, SchielW, Goldberg V, et al. Dish-stirling systems: an overview of development and status. J Solar Energy Eng 2003; 125(2): 135-51.
[5]. A. Gama, M. Haddadi, A. Malek; 2008; Etude et réalisation d'un concentrateur cylindro parabolique avec poursuite solaire aveugle; PP437 – 451.
[6]. Trading Economics, Banque mondiale, 2021
[7]. Union économique et monétaire ouest-africaine (UEMOA), « "Enquête harmonisée sur les conditions de vie des ménages" (EHCVM) dans l'UEMOA », 24 juillet 2020.
[8]. Pierre-Marie Cussaguet, « Le Niger, laboratoire de l'électrification durable en Afrique subsaharienne? », Briefings de l'Ifri, Ifri, 18 octobre 2021.
[9]. Rapport d'activité 2020, Autorité de régulation du secteur de l'énergie (ARSE).
[10]. Convention entre l'État nigérien et Istithmar. La centrale de Goudel 89 MW a démarré son activité en mars 2021. La construction de la centrale de Zinder 22 MW a débuté en août 2021.
[11]. https://www.univ-chlef.dz/ft/wp-content/uploads/2020/10/Chapitre-2.pdf, 17 04 2023, 18h 28.
[12]. Alain Ricaud; Gisement solaire et transferts énergétiques ; Université de CERGY-PONTOISE, jan 2011, P79.
[13]. Abdou Lawane a, Jacques Rémy Minane b, Raffaele Vinai c, ∗, Anne Pantet ; 2019 ; Mechanical and physical properties of stabilised compressed coal bottom ash blocks with inclusion of lateritic soils in Niger.
[14]. Djika Seydou, 2022, Evaluation du potentiel solaire thermodynamique aux environs de centre d'enfouissement de mâchefer de SONICHAR à Tchirozérine, Master, FAST UAM, P67.
[15]. Direction Régionale de l'environnement d'Agadez-Niger.
[16]. Mansouri Nadir; Makhloof Azwaw (2021); Dimensionnement thermique d'un récepteur solaire à tour à génération directe de vapeur, Master; P101.
[17]. Harouna, S., Abdoulaye, B., Mariama,P., Makinta,B. & Saïdou, M.(2022), Etude de Quatre (4) Modèles Semi-Empiriques d'Estimation du Rayonnement Solaire Direct et de Modélisation pour Application au Système Solaire Thermodynamique; European Journal of Applied Sciences (EJAS). P766-782.
[18]. Jean Marc VALLEE et Florence TROUILLET; Mesure de la constante solaire, IFE, 19/09/2017.
[19]. Emeric TAPACHÈS, 2016; Estimation du Potentiel de la Technologie Solaire Thermodynamique à Concentration en Climat Non Désertique - Application à La Réunion; Thèse de Doctorat, Universite De La Reunion; P217.
[20]. M. Hamdani, S.M.A. Bekkouche, T. Benouaz, ET M.K. Cherier; 2011; étude et modélisation du potentiel solaire adéquat pour l'estimation des éclairements incidents à Ghardaïa; P8-13.
[21]. M. Koussa, A. Malek, M. Haddadi; 2006; Validation de quelques modèles de reconstitution des éclairements dus au rayonnement solaire direct, diffus et global par ciel clair; P307 – 332.
[22]. Emmanuel Wendsongré Ramdé, Yao Azoumah, Abeeku Brew-Hammond, Anselme Rungundu, Gildas Tapsoba, 2013, Site Ranking and Potential assessment for Concentrating Solar Power in West Africa, Natural ressources. P. 146-153.